

# Structural Health Monitoring of Buildings Using Smartphone Sensors

by Qingkai Kong, Richard M. Allen, Monica D. Kohler, Thomas H. Heaton, and Julian Bunn

## ABSTRACT

This article presents the results of a shaker test of the Millikan Library in Pasadena, California, using sensors inside smartphones to demonstrate their potential usage as a way to monitor health states of buildings. This approach to structural health monitoring could allow many more commercial and residential buildings to be monitored because it removes the cost prohibitive nature of traditional seismic arrays and the complexity of deploying the instruments. Recordings from the smartphones during the shaking show high correlation with those from a reference sensor in the building, illustrating that the phones can capture the shaking even when not fully coupled to the floor. The fundamental translational frequencies for the east–west and north–south directions and the torsional frequencies of the building can be extracted from single phone recordings. As we compare the displacement derived from the phone recording by double integration to that from the reference sensor, both phase and amplitude match well. Signal-to-noise ratio is improved further by stacking records from multiple phones. These test results demonstrate the ability to extract the fundamental translational and torsional frequencies, and absolute displacements from upper levels of buildings shaken by small local earthquakes. This work builds on the ongoing MyShake project—a global smartphone seismic network.

*Electronic Supplement:* Time and frequency domain response of records.

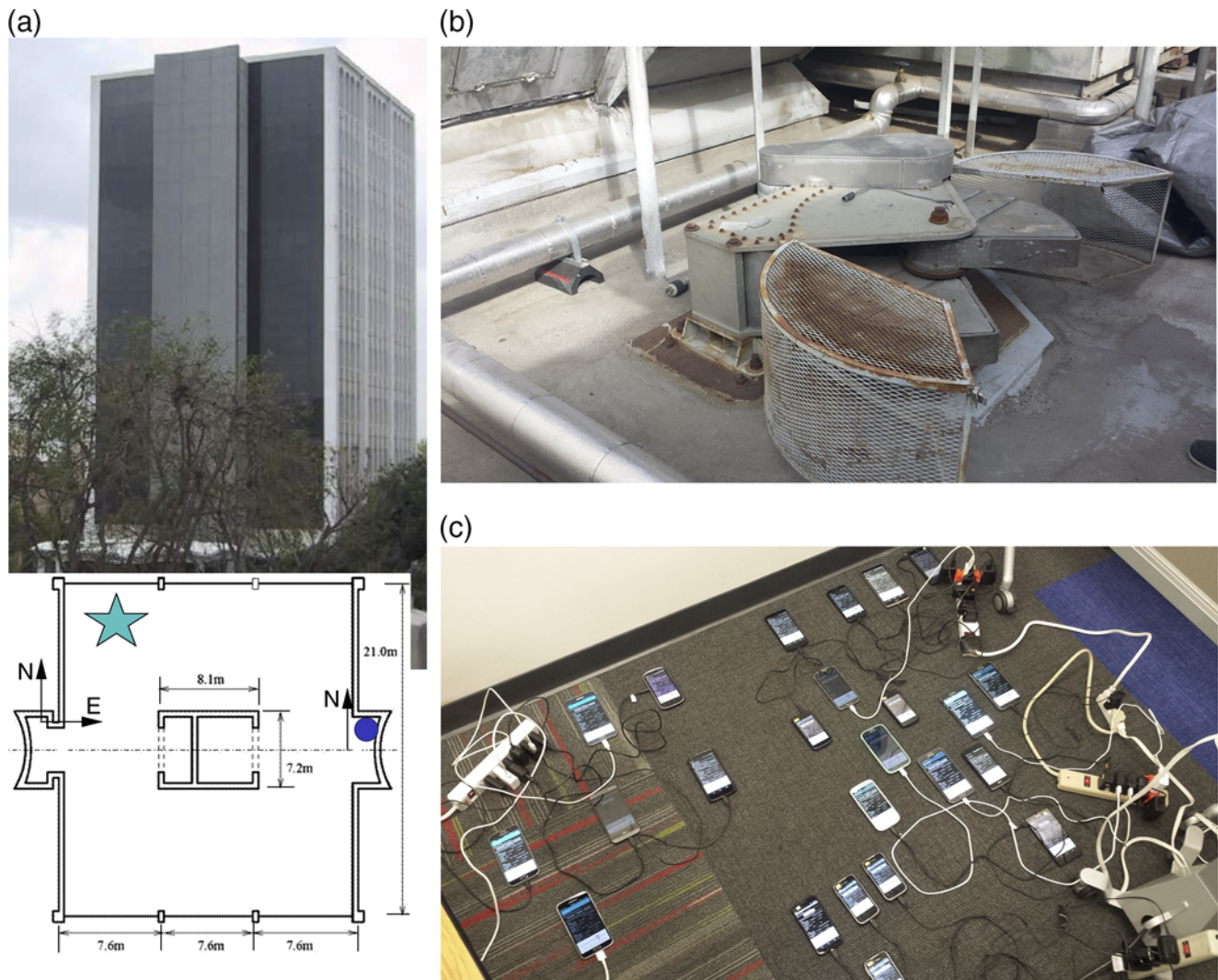
## INTRODUCTION

Structures such as buildings, bridges, roads, and dams are an essential part of modern society. Even though they are designed to be used in different conditions, extreme unpredictable events, that is, earthquakes, hurricanes, as well as deterioration due to aging, can cause serious concerns about the safety and functionality of the structures. Therefore, there is a need to monitor the health states of the structures throughout their lifetime.

Structural health monitoring (SHM) is a process that involves, first, observing a structural or mechanical system over time using periodically spaced measurements; second, extracting the damage-sensitive features from these measurements; and third, statistically analyzing these features to determine the current state of system health (Farrar and Worden, 2007). Different types of sensors are deployed in the structures either permanently or temporarily to extract measurements such as acceleration, velocity, displacement, deformation, stress, and temperature (Moreno-Gomez *et al.*, 2017). SHM is expensive both in terms of the hardware and the human effort; it is implemented in only a few large-scale structures, and must currently be deployed and maintained by practicing structural engineering professionals. Therefore, it is virtually impossible to conduct continuous long-term monitoring of the state of health of most buildings due to the cost of both hardware and human efforts.

The emergence of wireless sensors, low-cost microelectro mechanical systems (MEMS) sensors, and sensor networks has started to provide lower cost solutions to replace traditional tethered monitoring systems (Xu *et al.*, 2004; Paek *et al.*, 2005; Lynch and Loh, 2006; Kim *et al.*, 2007; Kohler *et al.*, 2013; Yin *et al.*, 2016). But to use them in a nationwide effort or even at the city level would require a large-scale effort for engineers to deploy and maintain these systems. In addition, many building owners are reluctant to install sensors in their buildings as they are fearful of legal issues or simply choose not to prioritize their building performance problems.

MyShake aims to build a global smartphone seismic network by utilizing the power of crowdsourcing. It turns an everyday handheld device into a portable seismometer by monitoring data from the accelerometer in a smartphone to detect earthquakes (Kong *et al.*, 2015; Kong, Allen, Schreier, *et al.*, 2016). After the release of the MyShake app to the public on 12 February 2016, it has been downloaded by more than 270,000 users globally. Today, about 10,000 active phones contribute data to the system each day for monitoring earthquakes. The results from the collected data are promising (Kong, Allen, and Schreier, 2016); MyShake can record M 5 earthquakes up to about 200 km from the smartphone, and it



▲ **Figure 1.** (a) The Millikan Library building viewed from the northeast. The two dark colored panels on the near-side of the building comprise the east shear wall (modified from [Bradford \*et al.\*, 2004](#)). The inset figure (modified from [Clinton \*et al.\* \(2006\)](#)) shows the plan of the building, where the star is the location of the test phones and the dot is the location of the Episensor station CI MIK. (b) The shaker located on the roof, used to generate oscillation of the building. The two exposed buckets contain lead masses that spin in opposite directions to generate a sinusoidal horizontal force. (c) The 25 smartphones used in the test, all placed on the floor of the ninth (top level) floor. The duration of the shaking in the north–south (N–S) direction is 1:29–3:02 p.m., and in the east–west (E–W) direction is 3:38–5:03 p.m., local time. The color version of this figure is available only in the electronic edition.

can record small magnitude earthquakes ( $M \geq 2.5$ ) at closer distances.

The quality of the data recorded by MyShake, and the ease of building and scaling up with this network, led us to investigate whether we might expand the use of MyShake data to the area of SHM. If private smartphone sensors can be used as a mechanism to collect data on the health state of buildings, then smartphones could overcome the substantial challenge of deploying the sensors manually in buildings, and provide a way to monitor the buildings at very low cost of hardware and maintenance. Because the smartphones may also be located throughout a building, this approach could provide a dense in-building network to monitor the structural health state of the building floor by floor.

Multiple groups studied the feasibility of using a low-cost sensor network to conduct SHM ([Cochran \*et al.\*, 2009](#); [Clayton \*et al.\*, 2011, 2015](#); [Kohler \*et al.\*, 2013, 2016](#); [Yin \*et al.\*, 2016](#)). These studies use specially designed low-cost sensor boxes that can be deployed in a building either by professional engineers or community volunteers. These sensors cost tens of dollars to a few hundred dollars each, but the more significant cost is associated with the fact that someone must manually deploy the sensors in buildings. This makes it challenging to scale up these networks due to the human labor, permitting, and permission efforts required.

In our study, smartphones provide an opportunity to replace this manual deployment process with a straightforward software download and installation onto the user's phone. In a

typical smartphone, a built-in three-axis accelerometer measures the movement of the phone in three dimensions (one vertical and two orthogonal horizontal components if the phone is oriented with one side parallel to the ground). Previous shake table tests of the accelerometers inside smartphones have shown that typical high-end accelerometers (used in iPhones and high-end Android phones) are capable of recording motion in the 0.2–20 Hz frequency range and 10–2000 mg amplitude range ( $g$  is gravitational acceleration) (D'Alessandro and D'Anna, 2013; Reilly *et al.*, 2013; Dashti *et al.*, 2014; Kong, Allen, Schreier, *et al.*, 2016). Engineers explored the use of smartphone sensors to monitor the health states of large-scale structures such as bridges. Yu *et al.* (2015) conducted a series of tests to show that using smartphones to carry out health monitoring of bridges is feasible. Ozer *et al.* (2015) and Feng *et al.* (2016) show that using smartphones attached to a pedestrian bridge, they can infer modal parameters from the recordings of the phones and layout of a structure for a crowdsourcing platform.

Here we explore the use of private smartphones to monitor building health. This is the first step in investigating whether the existing global MyShake network of smartphones as well as similar crowdsourcing smartphone efforts (Faulkner *et al.*, 2014; Finazzi, 2016) could be harnessed for this purpose, in addition to monitoring earthquake activity. We show results from a shaker test of the Millikan Library building on the Caltech campus in which we placed the phones on the floor of the ninth (top level) floor. We determine if we can extract

the fundamental frequencies of the building, and estimate the displacement of the floor due to motions similar to that from a small, nearby earthquake. Personal smartphones are, of course, in motion with their owners for portions of the day as the owner walks, commutes, etc. Our test is similar to the results expected for stationary phones resting on stands at night, or when placed on a desk or left in a bag on the floor. The results presented here illustrate the potential of using MyShake-enabled personal smartphones to record building shaking resulting from nearby earthquakes and using that data to extract the building characteristics. We also present a method to determine the orientation of the smartphone if its orientation is not known, but prior information about the building characteristics is available.

## BACKGROUND OF MILLIKAN LIBRARY

The shaker test was conducted at the Millikan Library building on the campus of the California Institute of Technology (Caltech) (Fig. 1a). Millikan Library is a nine-story, reinforced concrete building, ~44 m tall, and 21 m by 23 m in plan. The building has concrete moment frames in both the east–west (E–W) and north–south (N–S) directions. Shear walls on the east and west sides of the building provide most of the stiffness in the N–S direction, and shear walls in the central core provide added stiffness in both directions (Bradford *et al.*, 2004).

The Millikan Library building is instrumented with a permanent, dense array of uniaxial strong-motion sensors

**Table 1**  
**List of Smartphones Used in the Test**

Brand/Model	<i>N</i>	Accelerometer Type	Vendor	Maximum Range (m/s <sup>2</sup> )	Resolution (m/s <sup>2</sup> )
Samsung S3	1	MPL	InvenSense	19.6	$3.83 \times 10^{-2}$
Samsung S4*	2	K330	STMicroelectronics	19.6	$5.99 \times 10^{-4}$
Samsung S5*	1	MPU6500	InvenSense	19.6	$5.99 \times 10^{-4}$
Samsung S6*	1	MPU6500	InvenSense	19.6	$5.99 \times 10^{-4}$
Samsung Note2	2	LSM330DLC	STMicroelectronics	19.6	$9.58 \times 10^{-3}$
Samsung Note4	1	LCM20610	InvenSense	39.2	$1.20 \times 10^{-3}$
Samsung Note5*	1	K6DS3TR	STMicroelectronics	39.2	$1.20 \times 10^{-3}$
Samsung-Exhibit-II	1	BMA222	Bosch	19.6	$1.53 \times 10^{-1}$
Nexus 5	2	MPU6515	InvenSense	39.2	$1.20 \times 10^{-3}$
LG-G2*	1	LGE	STMicroelectronics	39.2	$1.20 \times 10^{-3}$
LG-G-Stylo	1	LGE	Bosch	156.9	$9.58 \times 10^{-3}$
LG-Leon*	1	LGE	Bosch	156.9	$9.58 \times 10^{-3}$
LG-G4	1	LGE	Bosch	156.9	$9.58 \times 10^{-3}$
HTC-One-M9	1	N/A	HTC Corp	39.2	$1.00 \times 10^{-2}$
MotoX	2	LIS3DH	STMicroelectronics	156.9	$4.79 \times 10^{-3}$
HuaWei Prism	3	BMA150	Bosch	39.2	$1.53 \times 10^{-1}$
Sony Xperia	2	MPL	InvenSense	19.6	$3.83 \times 10^{-2}$
HTC Amaze	1	Panasonic	Panasonic	19.6	$1.20 \times 10^{-2}$

Brand and model of the phones are shown; *N* is the number phones used in the test. Max Range and Resolution show the range of the amplitude and the smallest measurable value that the sensor can measure. The phones flagged with \* indicate that the phone is used in the seven-phone stack. The resolution values are from the sensor specifications.



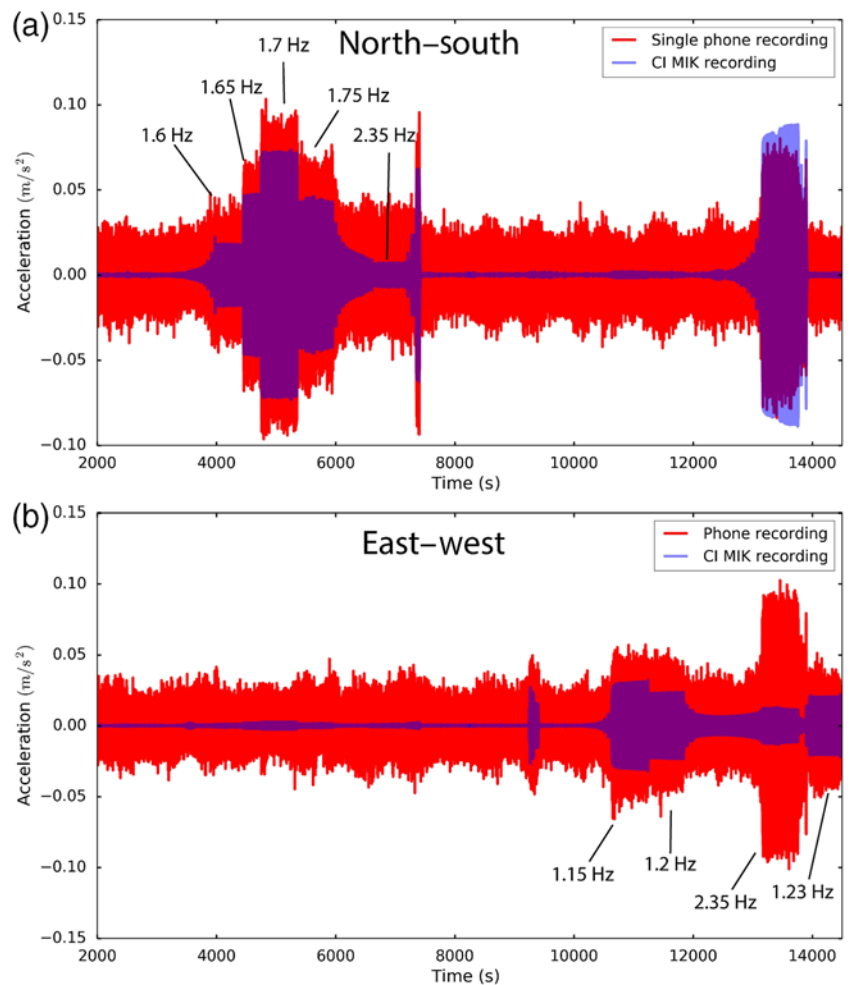
(Kinometrics FBA-11s in 1g and 2g) with 36 channels throughout the building. On each floor, there are three horizontal accelerometers; in addition, three vertical accelerometers are installed in the basement. A three-axis Episensor is installed on the ninth floor with a 24-bit data logger (Bradford *et al.*, 2004) (see the location in Fig. 1a). In addition, the building is instrumented with 10 Community Seismic Network accelerometers distributed on each floor (Kohler *et al.*, 2013). Previous studies have shown changes in the modal parameters of the building through time as a result of large-amplitude ground shaking (Clinton *et al.*, 2006). These studies illustrate the importance of understanding and documenting the dynamic properties of different classes of structures (i.e., steel-frame versus reinforced-concrete buildings) within the linear response regime before a nonlinear response might occur.

## METHOD

A Kinometrics model VG-1 synchronized vibration generator (shaker) was installed on the roof of Millikan Library in 1972 (Fig. 1b). The shaker has two buckets that rotate elliptically in opposite directions around a center spindle. These buckets can be loaded with different configurations of lead weights, and depending on the alignment of the buckets, the shaker can apply a sinusoidal force in any horizontal direction (Bradford *et al.*, 2004).

In our tests, we applied forces to the building first in the N-S direction, and then in the E-W direction at discrete frequencies. The applied frequencies of oscillation spanned 0.2–2.45 Hz and were varied gradually over the course of ~2.5 hrs. The rate of change of frequency varied over the course of the sweep. The sweep progressed at 0.05-Hz intervals with frequencies held constant for 60 s most of the time, but near the modal frequencies, the constant-frequency interval was extended to 600 s. The extended runtime was used for the building's fundamental E-W-mode frequency of 1.2 Hz, the fundamental N-S-mode frequency of 1.7 Hz, and the fundamental torsional-mode frequency of 2.4 Hz. Additional details of the test runs are provided in Table S1 (available in the electronic supplement to this article).

Smartphones were placed in the northwest corner of the ninth floor (top level) of Millikan Library (Fig. 1a,c) with their *x* axis approximately aligned in the E-W direction. For this test, the phones are placed at the most advantageous location, as the displacements on the corner of the ninth floor will be greater than at many other locations in the structure. Twenty-five different models of Android phones were tested (see Table 1 for



▲ **Figure 2.** Waveform comparisons between the Episensor (CI MIK) and a Samsung Galaxy S4 phone for the two horizontal components. (a) N-S component; (b) E-W component. Frequency labels indicate when the test run is at or near the fundamental or torsional frequencies of the building. The time for each test run can be found in Table S1 (available in the electronic supplement to this article). The amplitude and phase alignment is generally good (see Fig. S1 which expands the time window of 4820–4850 s). The color version of this figure is available only in the electronic edition.

details) as the accelerometers in Android phones are of various qualities (Kong, Allen, Schreier, *et al.*, 2016). The phones have flat response in the 0.1–12.5 Hz frequency range, and we use a sampling rate of 25 samples per second for these tests. The resolution listed in Table 1 is from the phone specifications and shows the best case when the phone is insulated from environmental vibrations.

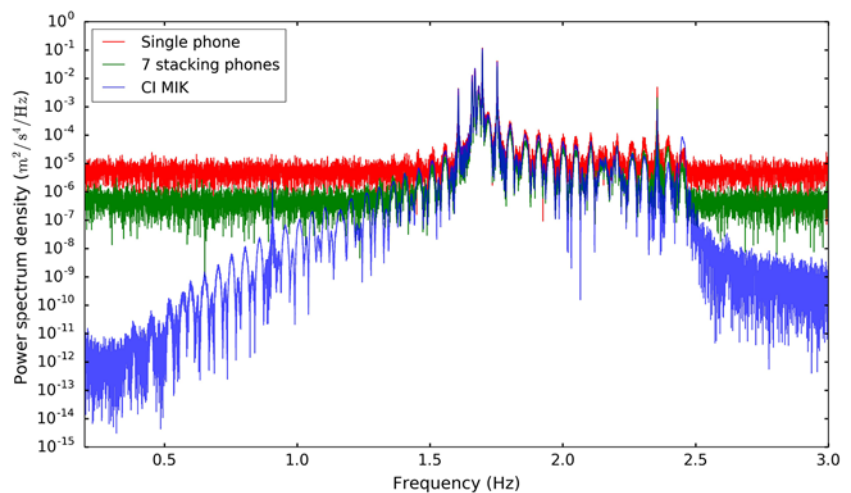
## RESULTS

Acceleration waveforms were recorded by the smartphones and compared to waveforms from a three-component Episensor, which is permanently installed on the ninth floor, to validate the smartphone motion. The Episensor has a 24-bit Q980 data logger, and its data are continuously telemetered to the

Southern California Seismic Network as station MIK. We will refer to it as station CI MIK in the following figures. Comparison of the acceleration waveforms between the Episensor and one of the Samsung Galaxy S4 phones is shown in Figure 2. The recording from the phone generally has a larger amplitude during peak shaking and a higher noise level that is above the lower amplitude shaking compared with the recording from CI MIK. Between times 2000–8000 s, the shaking was applied in the N-S direction, and from 9000–15,000 s it was applied in the E-W direction (Fig. 2). During each time interval, shaking was applied at a range of frequencies including the fundamental translational mode in that direction and the fundamental torsional mode that excites motion in both directions due to the rotational nature of torsion about a vertical axis. It is clear that the recordings from the phone and the Episensor from N-S and E-W shaking show good correlation, though the amplitude of the phone signal is greater than the Episensor. A shorter time window of the comparison is shown in ☉ Figure S1 illustrating the phase matching. The signals during the torsional motion (shaking frequency around 2.35 Hz), however, do not correlate in the same way, due to the different locations of the sensors on the ninth floor. At the location of the Episensor, the torsional motion is mainly in the N-S direction; the smartphones located at the northwest corner of the building, however, experienced motion in both the N-S and E-W directions, causing the amplitude difference. This can be seen in the time range from 13,000 to 14,000 s (Fig. 2).

Just one smartphone records building response to the shaking well, especially at the fundamental frequencies and torsional frequency. From the spectrum (Fig. 3), we clearly see the peak at the fundamental frequency and torsional frequency, and can thus extract them from a single phone. Because we have 25 smartphones at the same location we can also stack them to improve the signal-to-noise ratio. This assumes that noise recorded by different phones is truly random, and stacking across different phones will cancel the noise but not the coherent signals caused by the building's response to shaking.

Because the phones are not synchronized with each other (each phone has its own network time), we use cross correlation to find the best alignment of the recordings from different phones. We calculated the cross correlation of the entire N-S-component time series between different phone recordings and a base phone recording by shifting them within 120 s windows to find the maximum correlation coefficient. To get the best stack, we select the phones with different thresholds of the correlation coefficients. Correlation-coefficient thresholds of 0.6, 0.5, 0.4, and 0.3, resulted in stacks with 7, 10, 14, and 16 phones, respectively. The quality of the waveforms recorded is also variable due to the different accelerometers in the phones; thus, stacking more phones does not always improve the resulting waveform. By comparing the waveforms and spectra (more



▲ **Figure 3.** Spectrum comparisons in the N-S direction where the fundamental mode of the building is at 1.7 Hz and the fundamental torsion mode is at 2.35 Hz. Blue is spectrum for the Episensor (CI MIK), red is spectrum for a single phone (Samsung Galaxy S4), and the green spectrum is from the 7-phone stack. The modal peaks are clearly visible in all cases. The color version of this figure is available only in the electronic edition.

on this below), we conclude that stacking seven phones gives us the best results (the correlation coefficient is larger than 0.6). These seven phones are flagged with an asterisk in Table 1, and we see that most of them have the best accelerometers based on specification resolution. Figure 4 shows the comparison of the waveforms between the Episensor (CI MIK) and the stack of seven phones. We see that the stack amplitudes are a better match to those observed on CI MIK. The noise levels during low-amplitude shaking are lower, and the observed amplitudes during peak shaking are more similar.

The main goal of our shaker test is to extract the fundamental frequencies of the building from the phones and to compare them for accuracy with those of the Episensor. To calculate the spectrum of the building's shaking, we found that a multitaper spectrum analysis obtains better results than a direct fast Fourier transform. In the multitaper analysis, the time-series data to be analyzed is multiplied by a series of orthogonal tapers, and then Fourier transformed and squared to obtain the estimate of the power spectrum density (PSD). The orthogonal tapers will generate many independent estimates of the PSD instead of only one, and an average of them will suppress the random variance in the estimation (Prieto *et al.*, 2009). We select the N-S and E-W components individually, and apply the multitaper analysis. Figure 3 shows the amplitude spectrum for the recordings of the N-S component from the Episensor, a single phone, and the stacked phone time series. Overall, we observe that the single phone spectrum has a noise level around  $10 \times 10^{-5}$  and the stacked phone time series has a noise level of about  $10 \times 10^{-6}$ , which make the peaks around 1.25–1.5 Hz observable. However, the fundamental frequency in the N-S direction is clearly visible in all cases at 1.7 Hz. The fundamental torsional-mode frequency at 2.35 Hz is also distinguishable in all cases. The E-W-component spectrum produces similar results

and the peak of the fundamental frequency is clearly visible (see © Fig. S2 for the spectrum comparison for the E-W component).

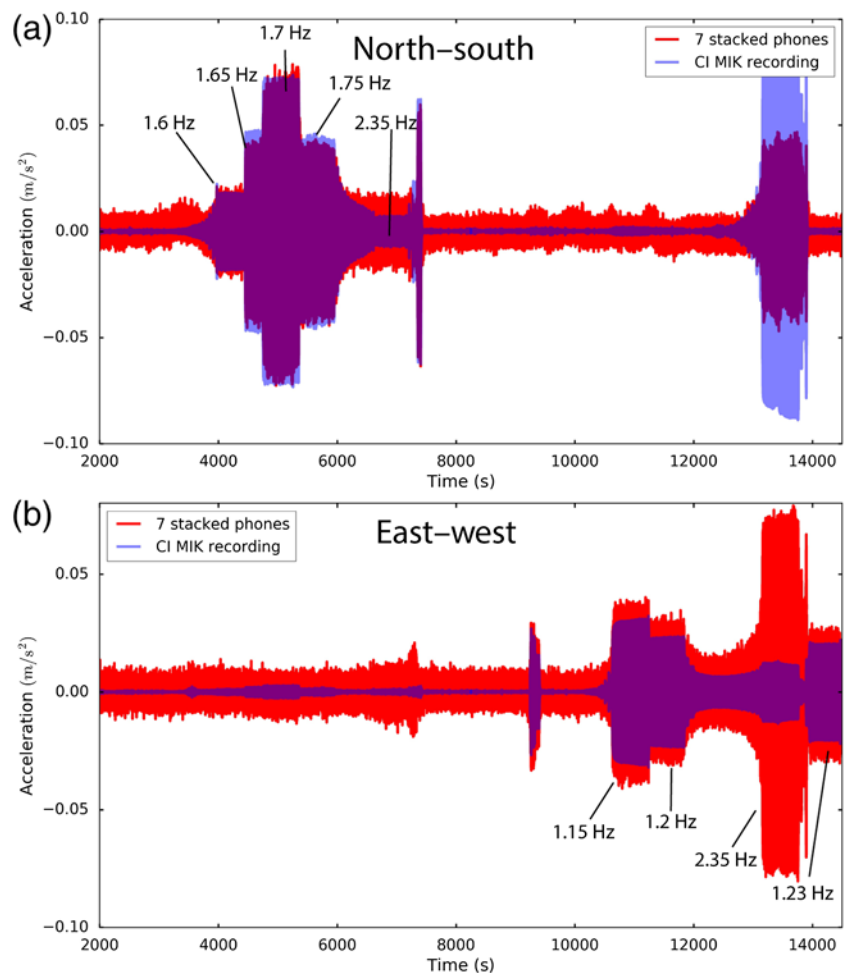
Peak and relative displacement amplitudes at a given floor of the building are also important to the civil engineering community to quantify localized deformation of the building (e.g., inter-story drift). In Figure 5, we show comparisons of the displacement time series between the Episensor, a single phone, and stacked phone recordings. Overall, the result from seven stacked phone time series shows better agreement with the Episensor in both phase and amplitude. These are obtained through double integration of the acceleration recordings by first removing the mean and trend in the record, and then applying a 0.5 Hz high-pass filter. They show good agreement with a peak displacement of about 0.05 cm for this frequency range.

## ESTIMATION OF THE ORIENTATION OF THE PHONES

Sometimes, we have the reverse problem in which we know the building's fundamental frequency but do not know the phone's orientation. If a building's modal frequencies and corresponding-mode shapes are already known, then it is possible to deduce the orientation of an arbitrarily rotated smartphone that is recording a known mode: rotate the phone until the resulting filtered motion is aligned with the mode shape. Analogous methods have been applied to find the orientation of three-component seismic sensors in various conditions (Duennebieer *et al.*, 1987; Ekstrom and Busby, 2008; Stachnik *et al.*, 2012). In our case, application of this method will only work for the translational model shapes, and when the phone produces a high signal-to-noise ratio recording, most likely from the free oscillations of the building following earthquake shaking. Also, the elevation of the phone is a factor as phones on the higher floors will likely have higher signal-to-noise ratio recordings.

Because we know that the N-S fundamental frequency of the Millikan Library building is 1.7 Hz, we should be able to estimate which component is N-S by applying a narrowband filter to the phone's two horizontal-component records. Figure 6 shows that the component shown in the top panel is likely close to the N-S direction; this is before any corrective rotation is applied. We observe that there is a small signal on the bottom-panel component as well, likely due to the fact that the phone is not perfectly oriented N-S during the tests.

To find the most accurate orientation of the phone during the tests, we can rotate the two horizontal components until an angle is found that minimizes the signal on one component. Figure 7 shows the result of rotating the phone 1.5°; the energy

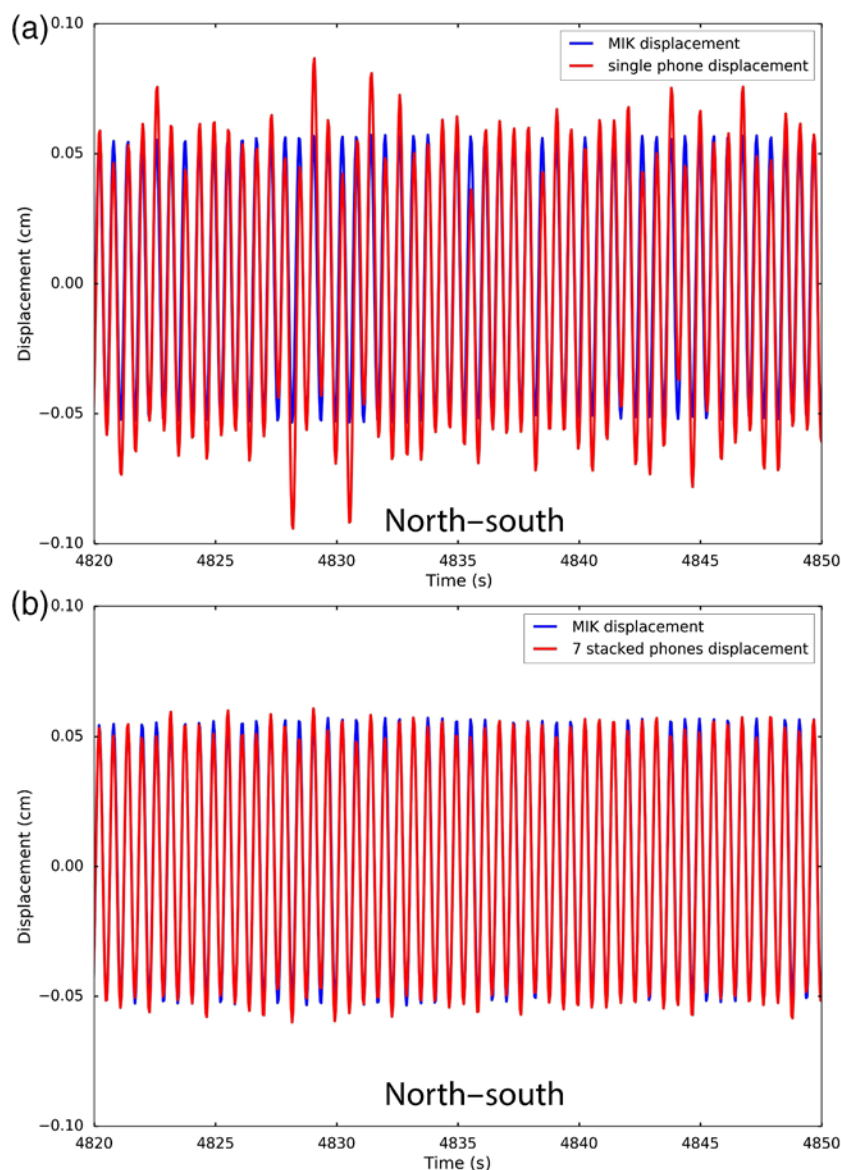


▲ **Figure 4.** Waveform comparisons for two horizontal components between the stack of seven phone recordings and the Episensor (CI MIK). (a) N-S component; (b) E-W component. Frequency labels indicate when the test run is at or near the fundamental or torsional frequencies of the building. The time for each test run can be found in © Table S1. The color version of this figure is available only in the electronic edition.

on the E-W component is minimized. Of course, this is easy for our test, because we shake the building in one direction at a time. During an earthquake, the later parts of the motion that are dominated by free vibrations should be usable in the same way to orient the phones. This will allow more meaningful analysis of earlier parts of the record.

Although a building's mode may not already be known, in some cases it is possible to estimate modal properties from the known geometry of the building. In particular, many buildings are approximately rectangular and the orientation of the building's normal modes is approximately aligned with the natural axes of the building. If structural design information is available to determine the most compliant direction of building deformation, then one can assume that the lowest-frequency normal mode of a building is also aligned with this direction. Even if the axis of the lowest frequency mode is unknown, it is often safe to assume that it is one of the two natural axes of the building. Knowing which of the two axes is the correct one can





▲ **Figure 5.** Displacement time-series comparisons (high-pass filtered at 0.5 Hz). These recordings are extracted from the period of largest-amplitude response to the shaking that occurred in the N-S direction, between 4820 and 4850 s (see Fig. 2a for reference). (a) The Episensor (CI MIK) compared with a single phone (Samsung Galaxy S4); (b) the Episensor compared with the seven-phone stack (see ⑤ Fig. S1 for the accelerations in the same time range). The color version of this figure is available only in the electronic edition.

be determined by observing the building's response with just one record of approximately known orientation (it is most beneficial to have at least one sensor with known orientation).

In some cases, tall buildings may have additional modes (overtones) at frequencies that are odd-integer multiples of the fundamental-mode frequency (Lee *et al.*, 2003). The orientations of higher modes can also be used to orient the phones. Finally, there are cases in which shear waves travel vertically up a building (typical wave velocity of 150 m/s). In general, the polarization of vertically propagating shear waves is approximately constant over the building height. If the

polarization of the incident wave is known, then the orientation of the phones can be determined by finding the appropriate rotation to reproduce the incident ground motion. Examples of how this is applied can be found in Cheng *et al.* (2015).

## DISCUSSION AND CONCLUSIONS

SHM is important for keeping track of the changes in the state of buildings, not only of large-scale structures but also of everyday residential buildings for the purpose of damage detection. Harnessing the smartphones of individual private users could open the door to monitoring many more structures including residential buildings in the future.

When compared with the current wireless sensor network monitoring systems, using consumer smartphones as a way to conduct SHM has the following benefits:

- ability to monitor millions of buildings within short periods of time;
- almost no cost for hardware and installation labor;
- low cost for long-term maintenance; and
- complementary data to the current monitoring system.

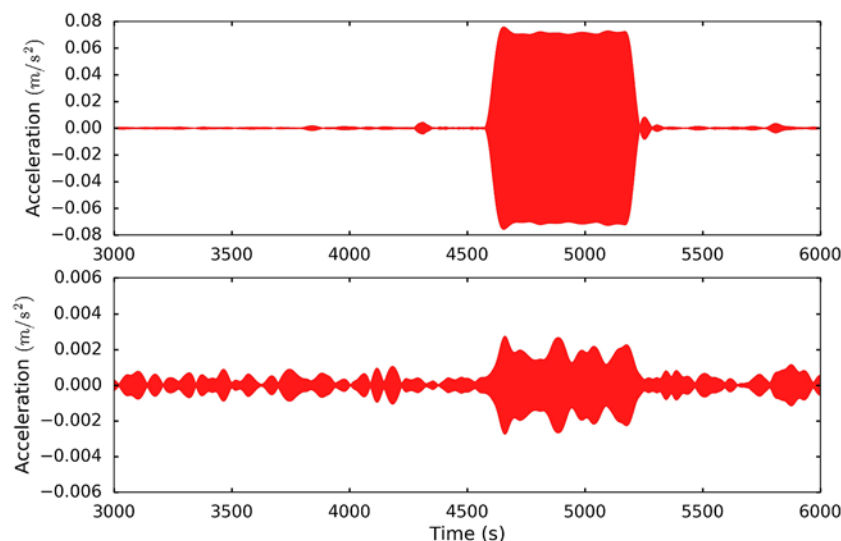
The first point is the most important benefit of using smartphones; millions of buildings could be monitored with just the download of an application. This will greatly improve our current monitoring ability at the city scale or even nation scale to reduce the earthquake risks. Also, a smartphone monitoring system is complementary to existing SHM systems by providing more data in the same building for validation and to fill in spatial sampling gaps.

This article is only a starting point for the concept of crowdsourcing SHM. There are still many challenges, including the following:

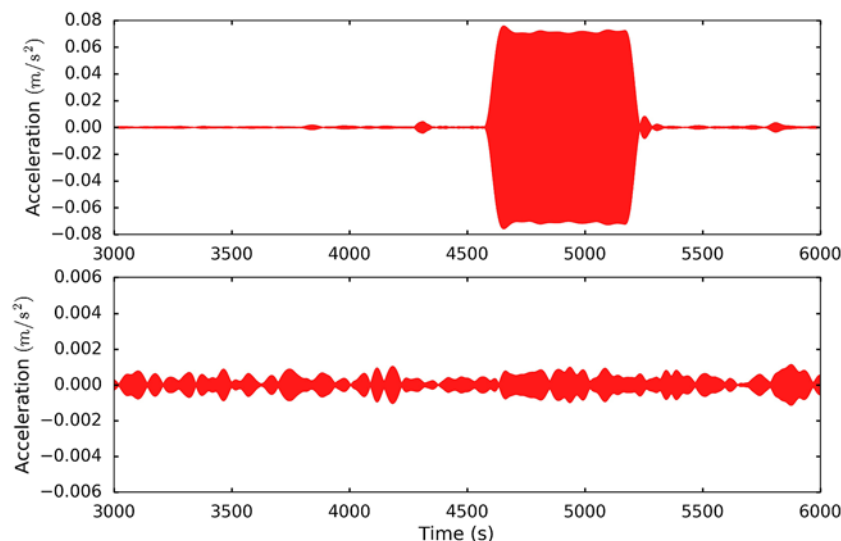
1. Determining accurate location, height (floor), and orientation of the phone is one of the biggest technical issues to solve.

There are several commercial solutions combining different sensors in the phones to get an estimate, but the results need to be tested. Another potential solution is to ask users to input their location and floor number after the earthquake into a questionnaire.

2. This test placed the phones in an ideal location, that is, on the top floor at the corner of the building with the phones lying on the floor. In reality, only a few phones may satisfy these requirements. Testing of phones on different floors, in different locations, and on different surfaces (desk, couch, etc.) is also necessary.



▲ **Figure 6.** Horizontal-component recordings after application of a narrow-band filter 1.69–1.71 Hz. Energy can be seen on both components. The upper panel is the component oriented roughly N-S, and bottom panel is the component oriented roughly E-W. The phone used here is the same Samsung Galaxy S4 as the one shown in Figure 2. The color version of this figure is available only in the electronic edition.



▲ **Figure 7.** Result of rotating the horizontal components of the narrow-band filtered signal (Fig. 6) anticlockwise 1.5° to minimize energy on one component. The upper panel shows the axis aligned to N-S after having rotated the components; the lower panel is the axis aligned to E-W. The color version of this figure is available only in the electronic edition.

3. Tests in different building types will also provide more insight into the types of information we can extract from the phone records for different buildings.
4. Making use of ambient vibrations of the building and nearby small earthquakes to extract a building's characteristic parameters will expand the capability of SHM from the phones. More work is needed to determine if ambient noise recordings could be recovered from phones and the lower

limits of earthquake shaking that can provide useful recordings.

These challenges illustrate that much research is needed before we can have a fully operational crowdsourced SHM system. However, the initial tests shown here illustrate the promise of using smartphones for SHM of buildings, and provide the basis for this future development of MyShake functionality.

## DATA AND RESOURCES

Data for the shaker tests are available via request to [rallen@berkeley.edu](mailto:rallen@berkeley.edu). ☒

## ACKNOWLEDGMENTS

This project is funded by Deutsche Telecom Silicon Valley Innovation Center, and by the Gordon and Betty Moore Foundation through Grant GBMF5230 to UC Berkeley. In the analysis of the data, ObsPy (Beyreuther *et al.*, 2010; Megies *et al.*, 2011) and mtspec package were used (doi: [10.5281/zenodo.321789](https://doi.org/10.5281/zenodo.321789)); we thank the authors. We also thank Lucy Yin, Anthony Massari, Kenny Buyco, and other students and staff for setting up the shaker tests. The authors thank the four anonymous reviewers; their comments greatly improved this article.

## REFERENCES

- Beyreuther, M., R. Barsch, L. Krischer, T. Megies, Y. Behr, and J. Wassermann (2010). ObsPy: A python toolbox for seismology, *Seismol. Res. Lett.* **81**, no. 3, 530–533, doi: [10.1785/gssrl.81.3.530](https://doi.org/10.1785/gssrl.81.3.530).
- Bradford, S. C., J. F. Clinton, J. Favela, and T. H. Heaton (2004). *Results of Millikan Library Forced Vibration Testing*, Technical report, California Institute of Technology, available at <http://resolver.caltech.edu/CaltechEERL:EERL-2004-03> (last accessed December 2017).
- Cheng, M. H., M. D. Kohler, and T. H. Heaton (2015). Prediction of wave propagation in buildings using data from a single seismometer, *Bull. Seismol. Soc. Am.* **105**, no. 1, 107–119, doi: [10.1785/B0120140037](https://doi.org/10.1785/B0120140037).
- Clayton, R. W., T. Heaton, M. Chandy, A. Krause, M. Kohler, J. Bunn, R. Guy, M. Olson, M. Faulkner, M. H. Cheng, *et al.* (2011). Community seismic network, *Ann. Geophys.* **54**, no. 6, 738–747, doi: [10.4401/ag-5269](https://doi.org/10.4401/ag-5269).
- Clayton, R. W., T. Heaton, M. Kohler, M. Chandy, R. Guy, and J. Bunn (2015). Community seismic network: A dense array to sense earthquake strong motion, *Seismol. Res. Lett.* **86**, no. 5, 1354–1363, doi: [10.1785/0220150094](https://doi.org/10.1785/0220150094).
- Clinton, J. F., S. C. Bradford, T. H. Heaton, and J. Favela (2006). The observed wander of the natural frequencies in a structure, *Bull. Seismol. Soc. Am.* **96**, no. 1, 237–257, doi: [10.1785/B0120050052](https://doi.org/10.1785/B0120050052).



- Cochran, E., J. Lawrence, C. Christensen, and R. S. Jakka (2009). The Quake-Catcher Network: Citizen science expanding seismic horizons, *Seismol. Res. Lett.* **80**, no. 1, 26–30, doi: [10.1785/gssrl.80.1.26](https://doi.org/10.1785/gssrl.80.1.26).
- D'Alessandro, A., and G. D'Anna (2013). Suitability of low-cost three-axis MEMS accelerometers in strong-motion seismology: Tests on the LIS331DLH (iPhone) accelerometer, *Bull. Seismol. Soc. Am.* **103**, no. 5, 2906–2913, doi: [10.1785/0120120287](https://doi.org/10.1785/0120120287).
- Dashti, S., J. D. Bray, J. Reilly, S. Glaser, A. Bayen, and E. Mari (2014). Evaluating the reliability of phones as seismic monitoring instruments, *Earthq. Spectra* **30**, no. 2, 721–742, doi: [10.1193/091711EQS229M](https://doi.org/10.1193/091711EQS229M).
- Duennebie, F. K., P. N. Anderson, and G. J. Fryer (1987). Azimuth determination of and from horizontal ocean bottom seismic sensors, *J. Geophys. Res.* **92**, no. B5, 3567–3572, doi: [10.1029/JB092iB05p03567](https://doi.org/10.1029/JB092iB05p03567).
- Eksstrom, G., and R. W. Busby (2008). Measurements of seismometer orientation at USArray transportable array and backbone stations, *Seismol. Res. Lett.* **79**, no. 4, 554–561, doi: [10.1785/gssrl.79.4.554](https://doi.org/10.1785/gssrl.79.4.554).
- Farrar, C. R., and K. Worden (2007). An introduction to structural health monitoring, *Phil. Trans. Roy. Soc. A* **365**, no. 1851, 303–315, doi: [10.1098/rsta.2006.1928](https://doi.org/10.1098/rsta.2006.1928).
- Faulkner, M., R. Clayton, T. Heaton, K. M. Chandy, M. Kohler, J. Bunn, R. Guy, A. Liu, M. Olson, M. H. Cheng, et al. (2014). Community sense and response systems: Your phone as quake detector, *Comm. ACM* **57**, no. 7, 66–75, doi: [10.1145/2622633](https://doi.org/10.1145/2622633).
- Feng, G., Z. Li, B. Xu, X. Shan, L. Zhang, and J. Zhu (2016). Coseismic deformation of the 2015  $M_w$  6.4 Pishan, China, earthquake estimated from Sentinel-1A and ALOS2 data, *Seismol. Res. Lett.* **87**, no. 4, doi: [10.1785/0220150264](https://doi.org/10.1785/0220150264).
- Finazzi, F. (2016). The earthquake network project: Toward a crowd-sourced smartphone-based earthquake early warning system, *Bull. Seismol. Soc. Am.* **106**, no. 3, doi: [10.1785/0120150354](https://doi.org/10.1785/0120150354).
- Kim, S., S. Pakzad, D. E. Culler, J. Demmel, G. Fennes, S. Glaser, and M. Turon (2007). Health monitoring of civil infrastructures using wireless sensor networks, *Proc. 6th Int. Conf. Information Processing in Sensor Networks*, 254–263, doi: [10.1109/IPSIN.2007.4379685](https://doi.org/10.1109/IPSIN.2007.4379685).
- Kohler, M. D., T. H. Heaton, and M.-H. Cheng (2013). The community seismic network and quake-catcher network: Enabling structural health monitoring through instrumentation by community participants, *Proc. of SPIE - Int. Soc. Opt. Eng.* **8692**, 86923X, doi: [10.1117/12.2010306](https://doi.org/10.1117/12.2010306).
- Kohler, M. D., A. Massari, T. H. Heaton, H. Kanamori, E. Hauksson, R. Guy, R. W. Clayton, J. Bunn, and K. M. Chandy (2016). Downtown Los Angeles 52-story high-rise and free-field response to an oil refinery explosion, *Earthq. Spectra* **32**, no. 3, 1793–1820, doi: [10.1193/062315EQS101M](https://doi.org/10.1193/062315EQS101M).
- Kong, Q., R. M. Allen, and L. Schreier (2016). MyShake: Initial observations from a global smartphone seismic network, *Geophys. Res. Lett.* **43**, no. 18, doi: [10.1002/2016GL070955](https://doi.org/10.1002/2016GL070955).
- Kong, Q., R. M. Allen, L. Schreier, and Y.-W. Kwon (2016). MyShake: A smartphone seismic network for earthquake early warning and beyond, *Sci. Adv.* **2**, no. 2, e1501055, doi: [10.1126/sciadv.1501055](https://doi.org/10.1126/sciadv.1501055).
- Kong, Q., Y.-W. Kwony, L. Schreier, S. Allen, R. Allen, and J. Strauss (2015). Smartphone-based networks for earthquake detection, *15th International Conf. on Innovations for Community Services (IACS)*, IEEE, 1–8.
- Lee, W. H. K., H. Kanamori, P. C. Jennings, and C. Kisslinger (Editors) (2003). *International Handbook of Earthquake and Engineering Seismology. Part B*, Elsevier, Amsterdam, The Netherlands.
- Lynch, J. P., and K. J. Loh (2006). A summary review of wireless sensors and sensor networks for structural health monitoring, *Shock Vib. Dig.* **38**, no. 2, 91–128.
- Megies, T., M. Beyreuther, R. Barsch, L. Krischer, and J. Wassermann (2011). ObsPy—What can it do for data centers and observatories?, *Ann. Geophys.* **54**, no. 1, 47–58, doi: [10.4401/ag-4838](https://doi.org/10.4401/ag-4838).
- Moreno-Gomez, A., C. A. Perez-Ramirez, A. Dominguez-Gonzalez, M. Valtierra-Rodriguez, O. Chavez-Alegria, and J. P. Amezcua-Sanchez (2017). Sensors used in structural health monitoring, *Arch. Comput. Methods Eng.* 1–18, doi: [10.1007/s11831-017-9217-4](https://doi.org/10.1007/s11831-017-9217-4).
- Ozer, E., M. Q. Feng, and D. Feng (2015). Citizen sensors for SHM: Towards a crowdsourcing platform, *Sensors* **15**, no. 6, 14,591–14,614, doi: [10.3390/s150614591](https://doi.org/10.3390/s150614591).
- Paek, J., K. Chintalapudi, J. Caffrey, R. Govindan, and S. Masri (2005). A wireless sensor network for structural health monitoring: Performance and experience, *Embed. Netw. Sens.* 1–10, doi: [10.1109/EMNETS.2005.1469093](https://doi.org/10.1109/EMNETS.2005.1469093).
- Prieto, G. A., R. L. Parker, and F. L. Vernon (2009). A Fortran 90 library for multitaper spectrum analysis, *Comput. Geosci.* **35**, no. 8, 1701–1710, doi: [10.1016/j.cageo.2008.06.007](https://doi.org/10.1016/j.cageo.2008.06.007).
- Reilly, J., S. Dashti, M. Ervasti, J. D. Bray, S. D. Glaser, and A. M. Bayen (2013). Mobile phones as seismologic sensors: Automating data extraction for the iShake system, *IEEE Trans. Automat. Sci. Eng.* **10**, no. 2, 242–251, doi: [10.1109/TASE.2013.2245121](https://doi.org/10.1109/TASE.2013.2245121).
- Stachnik, J. C., A. F. Sheehan, D. W. Zietlow, Z. Yang, J. Collins, and A. Ferris (2012). Determination of New Zealand ocean bottom seismometer orientation via Rayleigh-wave polarization, *Seismol. Res. Lett.* **83**, no. 4, 704–713, doi: [10.1785/0220110128](https://doi.org/10.1785/0220110128).
- Xu, N., S. Rangwala, K. K. Chintalapudi, A. Broad, R. Govindan, and D. Estrin (2004). A wireless sensor network for structural monitoring, *Proc. 2nd International Conf. Embedded Networked Sensor System*, ACM, 3–5 November 2004, 13–24.
- Yin, R.-C., Y.-M. Wu, and T.-Y. Hsu (2016). Application of the low-cost MEMS-type seismometer for structural health monitoring: A pre-study, *2016 IEEE International Instrumentation and Measurement Technology Conf. Proc. IEEE*, 1–5.
- Yu, Y., R. Han, X. Zhao, X. Mao, W. Hu, D. Jiao, M. Li, and J. Ou (2015). Initial validation of mobile-structural health monitoring method using smartphones, *Int. J. Distrib. Sens. Networks* **11**, no. 2, Article ID 274391, doi: [10.1155/2015/274391](https://doi.org/10.1155/2015/274391).

**Qingkai Kong**  
 Berkeley Seismology Laboratory  
 University of California, Berkeley  
 289 McCone Hall  
 Berkeley, California 94720 U.S.A.  
[kongqk@berkeley.edu](mailto:kongqk@berkeley.edu)

**Richard M. Allen**  
 Berkeley Seismology Laboratory  
 University of California, Berkeley  
 279 McCone Hall  
 Berkeley, California 94720 U.S.A.

**Monica D. Kohler**  
**Thomas H. Heaton**  
 Civil and Mechanical Engineering  
 Caltech  
 MC: 104-44  
 Pasadena, California 91125 U.S.A.

**Julian Bunn**  
 109 Powell-Booth Computing Center  
 Caltech  
 MC: 158-79  
 Pasadena, California 91125 U.S.A.

Published Online 10 January 2018